S100A1 DNA-based Inotropic Therapy Protects Against Proarrhythmogenic Ryanodine Receptor 2 Dysfunction

Julia Ritterhoff[1], Mirko Völkers[1], Andreas Seitz[1], Kristin Spaich[1], Erhe Gao[2], Karsten Peppel[3], Sven T Pleger[1], Wolfram H Zimmermann[4,5], Oliver Friedrich[6], Rainer HA Fink[7], Walter J Koch[2], Hugo A Katus[1,8] and Patrick Most[1,3,8,9]

[1]Molecular and Translational Cardiology, Department of Internal Medicine III, Heidelberg University Hospital, Heidelberg, Germany; [2]Center for Translational Medicine, Department of Pharmacology, School of Medicine, Temple University, Philadelphia, Pennsylvania, USA; [3]Center for Translational Medicine, Department of Medicine, Thomas Jefferson University, Philadelphia, Pennsylvania, USA; [4]Institute of Pharmacology, Heart Research Center Göttingen, Georg-August-University Göttingen, Göttingen, Germany; [5]German Center for Cardiovascular Research (DZHK), partner site Göttingen, Göttingen, Germany; [6]Institute of Medical Biotechnology, University of Erlangen-Nürnberg, Erlangen, Germany; [7]Institute of Physiology and Pathophysiology, Medical Biophysics, University of Heidelberg, Heidelberg, Germany; [8]German Centre for Cardiovascular Research (DZHK), partner site Heidelberg/Mannheim, Heidelberg, Germany; [9]uniQure GmbH Germany, Heidelberg, Germany

Restoring expression levels of the EF-hand calcium (Ca^{2+}) sensor protein S100A1 has emerged as a key factor in reconstituting normal Ca^{2+} handling in failing myocardium. Improved sarcoplasmic reticulum (SR) function with enhanced Ca^{2+} resequestration appears critical for S100A1's cyclic adenosine monophosphate-independent inotropic effects but raises concerns about potential diastolic SR Ca^{2+} leakage that might trigger fatal arrhythmias. This study shows for the first time a diminished interaction between S100A1 and ryanodine receptors (RyR2s) in experimental HF. Restoring this link in failing cardiomyocytes, engineered heart tissue and mouse hearts, respectively, by means of adenoviral and adeno-associated viral S100A1 cDNA delivery normalizes diastolic RyR2 function and protects against Ca^{2+}- and β-adrenergic receptor-triggered proarrhythmogenic SR Ca^{2+} leakage *in vitro* and *in vivo*. S100A1 inhibits diastolic SR Ca^{2+} leakage despite aberrant RyR2 phosphorylation via protein kinase A and calmodulin-dependent kinase II and stoichiometry with accessory modulators such as calmodulin, FKBP12.6 or sorcin. Our findings demonstrate that S100A1 is a regulator of diastolic RyR2 activity and beneficially modulates diastolic RyR2 dysfunction. S100A1 interaction with the RyR2 is sufficient to protect against basal and catecholamine-triggered arrhythmic SR Ca^{2+} leak in HF, combining antiarrhythmic potency with chronic inotropic actions.

Received 30 October 2014; accepted 28 April 2015; advance online publication 30 June 2015. doi:10.1038/mt.2015.93

INTRODUCTION

Impaired sarcoplasmic reticulum (SR) calcium (Ca^{2+}) homeostasis emerged as a hallmark in human heart failure (HF). This defect may be involved in the pathogenesis of lethal ventricular tachyarrhythmias,[1–3] which account for almost half of the HF-related deaths.[4] Enhanced diastolic SR Ca^{2+} leakage through dysfunctional ryanodine receptors (RyR2) is recognized to provoke an inward sodium current via the sodium-calcium exchanger (NCX) forward mode, which predisposes to arrhythmogenic diastolic membrane depolarizations in remodeled myocardium.[5–7] Residual β-adrenergic receptor (βAR) responsiveness can exacerbate diastolic RyR2 dysfunction further lowering the threshold for arrhythmogenic SR Ca^{2+} leak.[8,9] Recent studies indicated a critical role of cyclic adenosine monophosphate (cAMP)-dependent signaling both in aberrant RyR2 phosphorylation and stoichiometry with accessory modulators, which may contribute to abnormal diastolic gating of the RyR2.[1,2,10] Hence, inotropic interventions in HF patients, which reload the SR with Ca^{2+} through direct or indirect manipulation of cAMP homeostasis, can come at the risk of enhanced SR Ca^{2+} leakage and mortality when used chronically.[11–14] Targeted improvement of SR Ca^{2+} handling through molecular interventions that can bypass cAMP-dependent pathways, however, emerged as a novel promising strategy for HF and might combine antiarrhythmic potency with the ability to chronically improve cardiac performance.[15] One such candidate might be S100A1, an EF-hand Ca^{2+} sensor protein that is highly expressed in cardiomyocytes (reviewed in refs. [16,17]). Diminished S100A1 protein expression, which is characteristic of advanced human HF, accelerates transition to contractile failure and exacerbates mortality in experimental HF models.[18–21] Restoring S100A1 expression in small and large animal HF models as well as in failing human cardiomyocytes by means of viral-based S100A1 cDNA delivery improved both systolic and diastolic contractile performance and reversed cardiac remodeling.[18,20,22–25] S100A1 seems to confer its therapeutic effect by associating with the SERCA2a/PLB complex and RyR2 in a Ca^{2+}-dependent manner,

The first two authors contributed equally to this work.

Correspondence: *Patrick Most, Molecular and Translational Cardiology, Department of Internal Medicine III, University of Heidelberg, INF 410, 69120 Heidelberg, Germany. E-mail: patrick.most@med.uni-heidelberg.de or Julia Ritterhoff, Molecular and Translational Cardiology, Department of Internal Medicine III, University of Heidelberg, INF 410, 69120 Heidelberg, Germany. E-mail: jr54@uw.edu*

both reloading the SR with Ca^{2+} and enhancing the excitation-contraction (EC) coupling gain in cardiomyocytes.[26] S100A1's molecular actions neither rely on βAR signaling nor involve downstream cAMP- or calmodulin (CaM)-dependent kinases.[19,20,26–28] Although a previous study indicated that S100A1 could decrease Ca^{2+} spark frequency in chemically permeabilized normal ventricular cardiomyocytes, the impact of S100A1 on diastolic RyR2 dysfunction in failing myocardium has not been determined yet.[29] Utilizing cellular, engineered heart tissue (EHT) and small animal HF models, our study shows for the first time that S100A1 can beneficially modulate diastolic RyR2 function in normal and failing ventricular cardiomyocytes, protect against βAR-triggered SR Ca^{2+} leak *in vitro* and lethal ventricular fibrillation (VF) *in vivo*. Restoring the diminished S100A1/RyR2 ratio in failing myocardium seems sufficient to reverse diastolic RyR2 dysfunction bypassing aberrant protein kinase A (PKA) and Ca^{2+}/CaM-dependent protein kinase II (CaMKII) phosphorylation as well as interaction with accessory modulators such as FKBP12.6, CaM or sorcin. Our data unveil novel mechanistic insights into therapeutic actions of S100A1 and bear the prospect of a molecular-targeted treatment against HF being translated towards clinical trials that combines antiarrhythmic with inotropic potency.

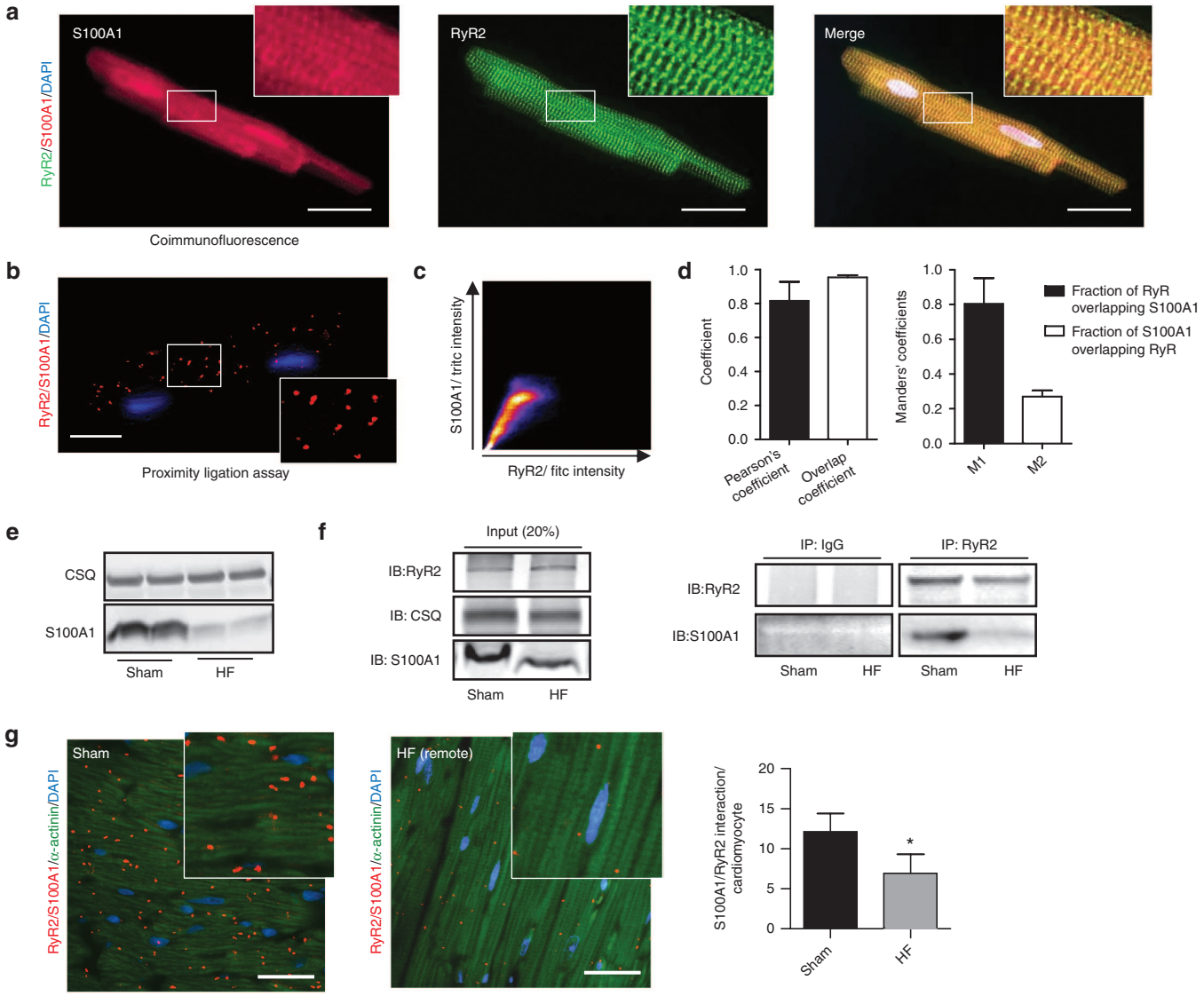

Figure 1 Diminished interaction between S100A1 and RyR2 in postischemic heart failure. (**a**) Representative immunofluorescent images for S100A1 (red) and RyR2 (green) in a normal left ventricular rat cardiomyocyte reveal partial colocalization of S100A1 with RyR2 (merged image, yellow). Inlet magnification is threefold. (**b**) Representative immunofluorescent PLA image depicts *in situ* S100A1/RyR2 association (red dots) in a left ventricular cardiomyocyte. Each dot represents a complex consisting of S100A1 and RyR2. Inlet magnification is twofold. (**c**) Representative scatterplot image from colocalization analysis of Figure 1a using the JACoP plugin from ImageJ. (**d**) Colocalization analysis from RyR2/S100A1, depicting Person's, Overlap and Mander's coefficients, $n = 3$. (**e**) Representative immunoblots show diminished S100A1 protein abundance in postischemic HF mouse hearts versus sham. CSQ served as loading control. (**f**) Left: Representative input immunoblot for RyR2 immunoprecipitation from sham and HF mouse hearts. Right: Representative immunoblots of immunoprecipitated RyR2 and coprecipitating S100A1 protein from sham and postischemic HF mouse hearts. (**g**) Comparative *in vivo* PLA for S100A1 and RyR2 in sham (left) and HF (right) murine myocardium. Cardiomyocytes were counterstained with α-actinin (green). Inlet magnification is twofold, $n = 3$. *$P < 0.05$ versus sham. Data are given as mean ± SEM. Cardiomyocyte nuclei were counterstained with 4',6-diamidino-2-phenylindole (DAPI; blue). Scale bar represents 20 µm.

RESULTS

S100A1 interaction with RyR2 is decreased in postischemic failing myocardium

Association of S100A1 with the RyR2 was first demonstrated in normal rat ventricular cardiomyocytes by coimmunofluorescence and proximity ligation assay (PLA) (**Figure 1a,b**). Colocalization analyses confirmed that the major fraction of RyR2 was associated with S100A1 (**Figure 1c,d**). On the other hand, only a subfraction of S100A1 was associated with the RyR2 (**Figure 1d**), in line with S100A1's different subcellular localizations and interacting partners (Sarcoplasmic reticulum, mitochondria, myofilmants; reviewed in ref. [16]). To investigate the interaction of S100A1 and RyR2 in failing hearts, myocardial infarction in C57BL/6 mice was performed that resulted in impaired cardiac performance after 2 weeks as demonstrated by left ventricular catheterization (**Supplementary Figure S1a**).[19] Left ventricular S100A1 protein levels were reduced compared to normal (sham-operated) mice (**Figure 1e**) and the RyR2/S100A1 interaction was also diminished as detailed by RyR2/S100A1 coimmunoprecipation (**Figure 1f**). Semiquantitative assessment of *in vivo* S100A1/RyR2 binding by PLA unveiled an approximately twofold reduction in the mouse HF model (**Figure 1g**). The novel finding prompted us to determine the impact of S100A1 on diastolic RyR2 function in quiescent normal (NCs) and failing (FCs) ventricular rat cardiomyocytes and to investigate a causal link between S100A1 and diastolic RyR2 activity.

S100A1 decreases RyR2-mediated SR Ca^{2+} leak in quiescent ventricular cardiomyocytes

Isolated rat normal cardiomyocytes (NCs) and failing cardiomyocytes (FCs) were subjected to *in vitro* AdGFP (control) and AdS100A1 (S100A1) transduction for 24 hours (**Supplementary Figure S2a–c**).[20] As expected, βAR stimulation in NCs and FCs resulted in augmented Ca^{2+} transient amplitudes and increased SR Ca^{2+} content (**Figure 2a**; **Supplementary Figure S1d**). A similar inotropic effect was seen after adenoviral-based S100A1 gene delivery (**Figure 2a**), resulting in an approximately threefold

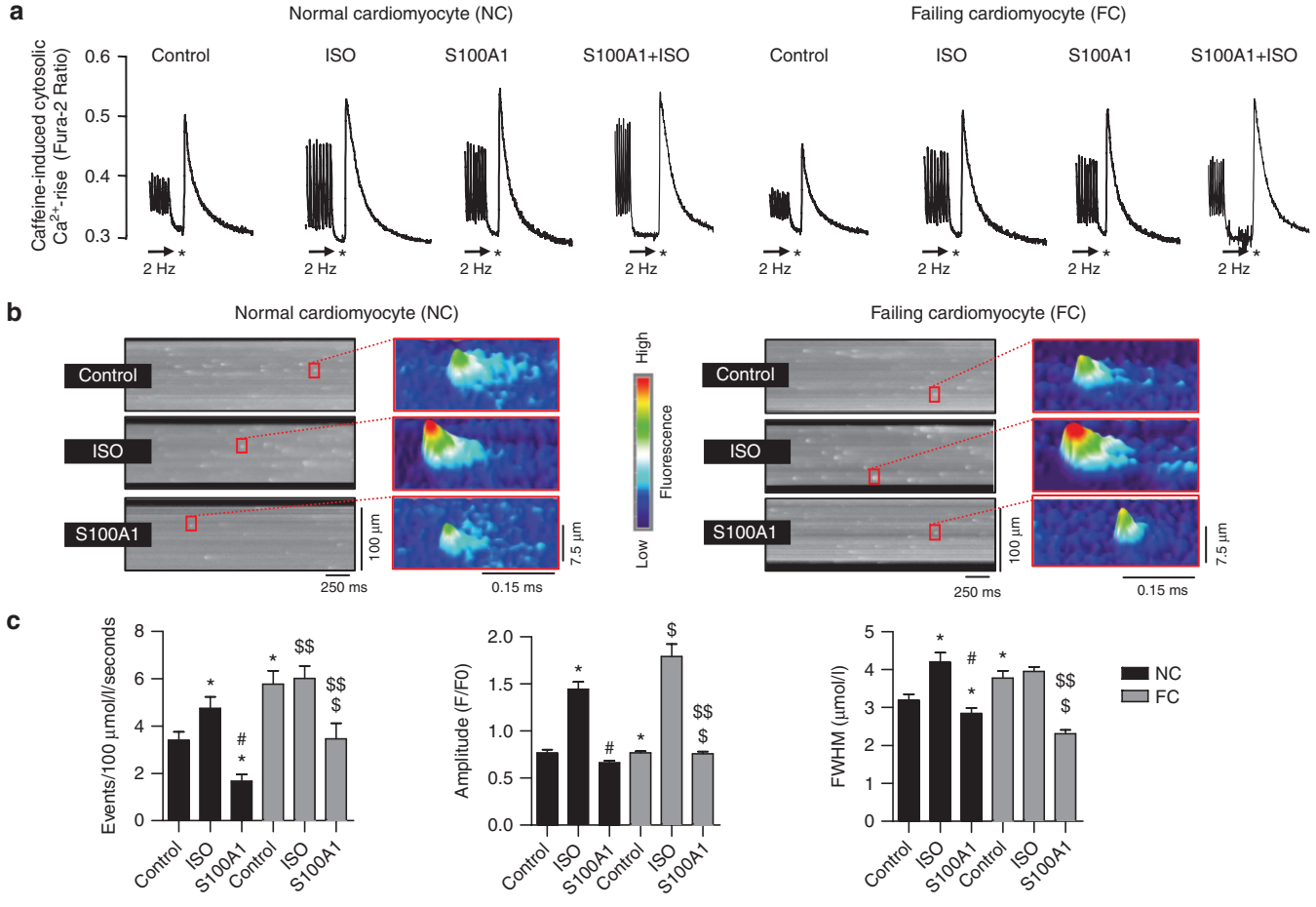

Figure 2 S100A1 attenuates physiological and abrogates pathological diastolic RyR2 activity. (**a**) Representative tracings of electrically-stimulated (2 Hz; arrow) steady-state Ca^{2+} transients from basal and ISO-stimulated (100 nmol/l) control (AdGFP) and S100A1-treated (AdS100A1) NCs (left) and FCs (right). Asterisk (*) indicates the 10 mmol/l caffeine pulse for semiquantitative assessment of the SR Ca^{2+} content due to the caffeine-mediated maximal rise of the cytosolic Ca^{2+} signal. Note that both ISO and S100A1 enhance the SR Ca^{2+} load in NCs and FCs (see **Supplementary Figure S1d** for statistical analyses). (**b**) Representative fluorescent line-scan and magnified surface plot images of elementary Ca^{2+} release events in control (AdGFP-transfected), isoproterenol-stimulated (ISO, 100 nmol/l, AdGFP-transfected) and S100A1 (AdS100A1-transfected) resting normal (NCs, left panel) and failing rat cardiomyocytes (FCs, right panel). (**c**) Corresponding statistical analysis of Ca^{2+} spark characteristics (frequency, amplitude, and width) shows that FCs exhibit significantly greater SR Ca^{2+} leak than NCs. S100A1 attenuates RyR2-mediated Ca^{2+} leak in NCs and FCs. $n = 90$ cells in each group derived from four different isolations. $^{*}P < 0.05$ versus NC control, $^{\#}P < 0.05$ versus NC ISO, $^{\$}P < 0.05$ versus FC control, $^{\$\$}P < 0.05$ versus FC ISO. Data are given as mean ± SEM.

increase in S100A1 protein expression in NCs and restoration of normal S100A1 protein levels in FCs (**Supplementary Figure S2a–d**). Resting conditions were then used to assess the impact of S100A1 and βAR stimulation (isoproterenol) on basal Ca^{2+} spark characteristics as an indicator of RyR2-mediated SR Ca^{2+} leak. Isoproterenol enhanced the leak both in quiescent NCs and FCs compared with control cells (**Figure 2b,c**). In contrast, S100A1-treated NCs exhibited a significant reduction in Ca^{2+} spark rate and S100A1 restoration in FCs effectively reversed abnormalities in diastolic RyR2 activity. Correlation analysis indicated a positive correlation of S100A1 protein levels from control and S100A1-treated normal and failing cardiomyocytes with Ca^{2+} transient amplitude ($r^2 = 0.87$) and SR Ca^{2+} load ($r^2 = 0.78$), whereas S100A1 protein levels displayed a negative correlation with Ca^{2+} spark frequency ($r^2 = 0.82$) (**Supplementary Figure S2e**). As expected, cultivation of CMs for 24 hours resulted in increased Ca^{2+} transient amplitude and reduced SR Ca^{2+} leak compared to freshly isolated CMs (2 hours after isolation) (**Supplementary Figure S2f**). Still, these data indicate a beneficial role for S100A1 in regulating diastolic RyR2 function which is different from the inotropic βAR agonist isoproterenol (**Figure 2b,c**). We next assessed whether the profound effect of S100A1 might rely on altered posttranslational modification of the RyR2 or stoichiometry with accessory molecules known to attenuate diastolic RyR2 activity.

Enhanced S100A1/RyR2 interaction alters neither RyR2 phosphorylation nor its interaction with accessory molecules

Isoproterenol stimulation yielded the expected increase both in PKA and CaMKII-dependent RyR2 phosphorylation at Ser-2808 and Ser-2814 (**Figure 3a**) and phospholamban (PLB) at Ser-16 and Thr-17 (**Supplementary Figure S3a**). *In vitro* AdS100A1 treatment interfered neither with PKA nor with CaMKII signaling (**Figure 3a**; **Supplementary Figure S3a**) under basal conditions and after βAR stimulation. Enhanced S100A1 protein levels increased S100A1/RyR2 binding approximately twofold compared to control (**Figure 3b,c**; **Supplementary Figure S3d**), assessed by different methods. Besides, activation of cAMP-dependent signaling did not change S100A1/RyR2 interaction compared to corresponding controls (**Figure 3b,c**; **Supplementary Figure S3d**). Furthermore, isoproterenol stimulation had no impact on the stoichiometry of the RyR2 with accessory modulators such as FKBP12.6 (**Figure 3d**), CaM or sorcin (**Supplementary Figure S3b,c**). Vice versa, augmented S100A1/RyR2 association did not interfere with RyR2 stoichiometry either. Thus, enhanced S100A1 binding to the RyR2 might directly account for improved diastolic RyR2 function in quiescent cardiomyocytes.

S100A1 prevents βAR-triggered compound Ca^{2+} sparks and Ca^{2+} waves in quiescent ventricular cardiomyocytes with leaky RyR2

As previous studies indicated that RyR2s in failing myocardium are sensitized to Ca^{2+}, which lowers the threshold for arrhythmic Ca^{2+} leak,[8,14] we investigated the impact of S100A1 on RyR2s chemically sensitized to cytosolic Ca^{2+}. We adopted a protocol to increase RyR2 open probability by low concentrations of caffeine (0.5 mmol/l).[8] Under these conditions, isoproterenol treatment resulted in a high rate of synchronized compound Ca^{2+} sparks (macrosparks) deteriorating into arrhythmic Ca^{2+} waves in 70 and 50% of quiescent NCs and FCs, respectively (**Figure 4a–d**). After S100A1 treatment, both NCs and FCs exhibited only solitary Ca^{2+} sparks and Ca^{2+} waves occurred with a significantly lower rate, indistinguishable from control (**Figure 4a–d**). Remarkably, S100A1 protected against βAR-induced Ca^{2+} waves due to a lowered incidence of Ca^{2+} sparks (**Figure 4a–d**). Besides, there was no interference of caffeine with S100A1 binding to RyR2 and RyR2 phosphorylation (**Supplementary Figure S4a–d**).

S100A1 inhibits βAR-triggered diastolic Ca^{2+} waves during EC coupling in ventricular cardiomyocytes with leaky RyR2

The marked effect of S100A1 in quiescent cells prompted the analysis of SR Ca^{2+} leak during EC coupling. When RyR2s were Ca^{2+} sensitized, addition of isoproterenol provoked premature diastolic Ca^{2+} waves (mean frequency of Ca^{2+} waves was 1.0 per Ca^{2+} transient) in more than 80% of NCs or FCs (**Figure 5a–d**). In contrast, both S100A1-expressing NCs and FCs showed no sign of diastolic SR instability. Importantly, enhanced S100A1 levels were highly effective in protecting cardiomyocytes during EC coupling against βAR-triggered arrhythmic SR Ca^{2+} leak (**Figure 5a–d**) during conditions when RyR2s were super-sensitized to Ca^{2+} both by caffeine and βAR stimulation.

S100A1 abrogates Ca^{2+}- and βAR-induced after-contractions and fibrillation in electrically coupled EHT

To determine whether S100A1-mediated prevention of Ca^{2+} waves translates into protection against diastolic after-contractions, we used ring-shaped rat EHTs to model 3-dimensional syncytial cardiac tissue. S100A1 staining in longitudinal syncytial cardiomyocyte bundles in EHTs resembled S100A1's subcellular distribution in matured rat ventricular cardiomyocytes (**Figure 6a**). In line with a previous study showing downregulation of S100A1 in cardiomyocytes by Gq-coupled receptor stimulation,[19] chronic ET-1 treatment (4 days) significantly reduced S100A1 protein levels by 50% (**Figure 6b**) and caused an HF-like phenotype characterized by impaired isometric twitch tension (**Figure 6c,d**). AdS100A1-treated normal EHTs (**Supplementary Figure S5a,b**) exhibited enhanced isometric contractility, while remodeled HF-like EHTs showed normalized contractile indices (**Figure 6c–e**) and Ca^{2+} responsiveness, respectively, after S100A1 gene delivery (**Supplementary Figure S5c**). Similarly, βAR stimulation by isoproterenol also resulted in enhanced isometric contractility (**Figure 6e**). Incremental extracellular Ca^{2+} concentrations, used to overload the SR with Ca^{2+}, triggered diastolic premature contractions, which deteriorated into fibrillation-like contractile patterns both in electrically stimulated (2 Hz) normal and HF-like EHTs (**Figure 6c,f,g**; **Supplementary Figure S5e**). Administration of ryanodine interrupted this pattern, indicating that improvement of RyR2 closure can abrogate SR Ca^{2+}-overload-induced after-contractions (**Supplementary Figure S5f–g**). S100A1 treatment significantly attenuated the incidence of Ca^{2+}-induced premature contractions and fibrillations in EHTs and the beneficial effect was even more pronounced in HF-like EHTs (**Figure 6f,g**).

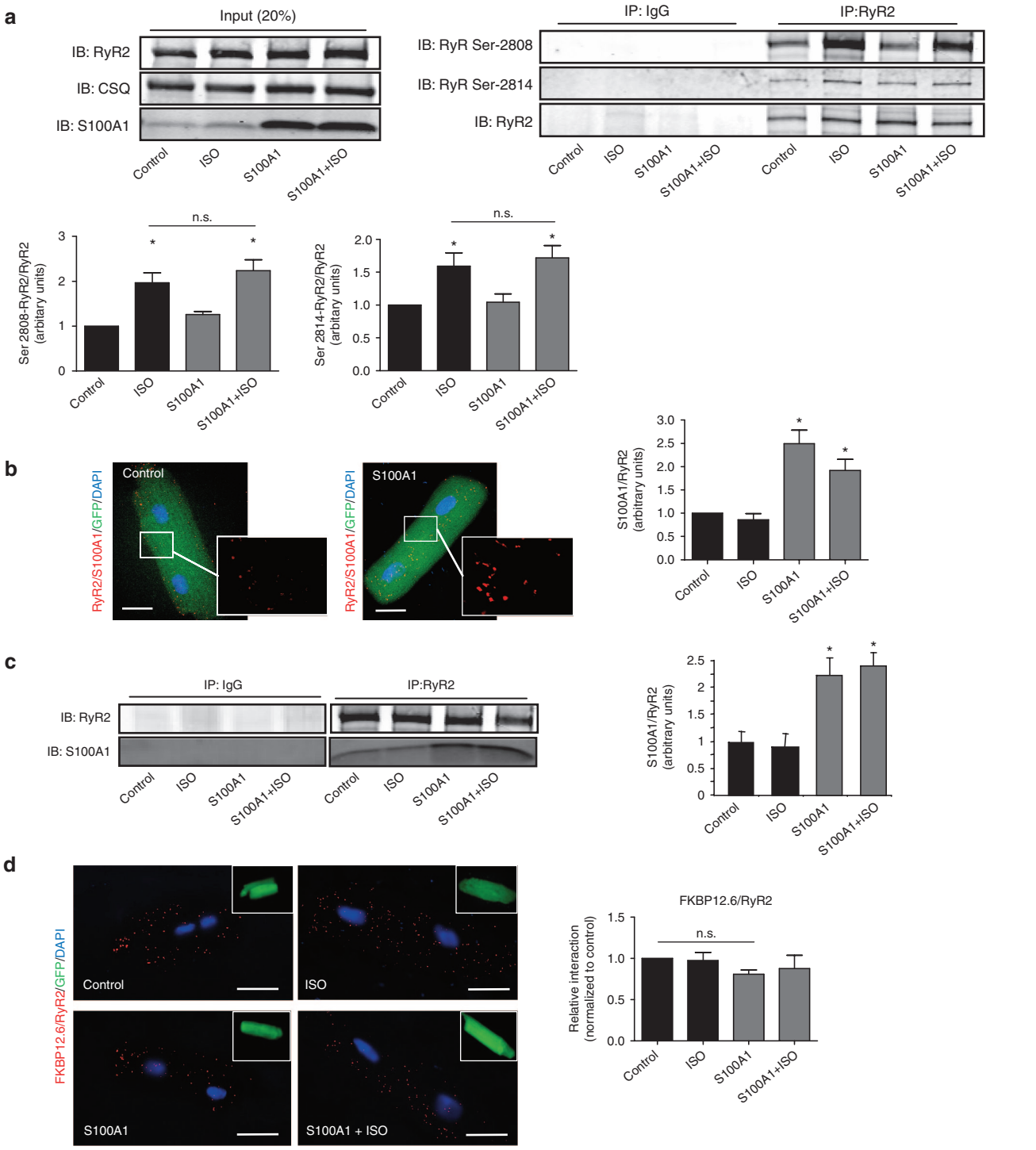

Figure 3 Enhanced S100A1/RyR2 binding does not alter RyR2 phosphorylation and interaction with accessory proteins. (**a**) Left: Representative input immunoblot for RyR2 immunoprecipitation from control and S100A1-treated NCs. Right: Representative immunoblot of immunoprecipitated RyR2 and corresponding immunoblot for total RyR2, Ser-2808, and Ser-2814 phosphorylation from basal and ISO-stimulated (100 nmol/l) control (AdGFP) and corresponding S100A1-expressing (AdS100A1) cardiomyocytes ($n = 5$). Quantification is shown below. (**b**) Representative PLA image from control (AdGFP) and S100A1-treated (AdS100A1) rat cardiomyocytes showing S100A1/RyR2 interaction (red dots). Inlet magnification is two-fold. Statistical analysis shows a twofold increase of the normalized arbitrary S100A1/RyR2 binding ratio ($n = 4$). (**c**) Representative immunoblot of immunoprecipitated RyR2 from basal and ISO-stimulated (100 nmol/l) control (AdGFP) and corresponding S100A1-expressing (AdS100A1) cardiomyocytes reveals a significant increase in coprecipitating S100A1 protein assessed by immunoblotting. Note that semiquantitative analysis of the normalized S100A1/RyR2 ratio matches results obtained with PLA ($n = 5$). (**d**) Representative PLA images for FKBP12.6/RyR2 interaction (red dots) in indicated groups. Inlets show the corresponding GFP-positive cardiomyocytes. Note that enhanced S100A1/RyR2 association did not change FKBP12.6 binding to the RyR2 ($n = 4$). Similar results were obtained for CaM and sorcin (**Supplementary Figure S3b,c**). *$P < 0.05$ versus control. Data are given as mean ± SEM. Nuclei (blue) were counterstained with 4',6-diamidino-2-phenylindole (DAPI). Scale bar represents 20 µm.

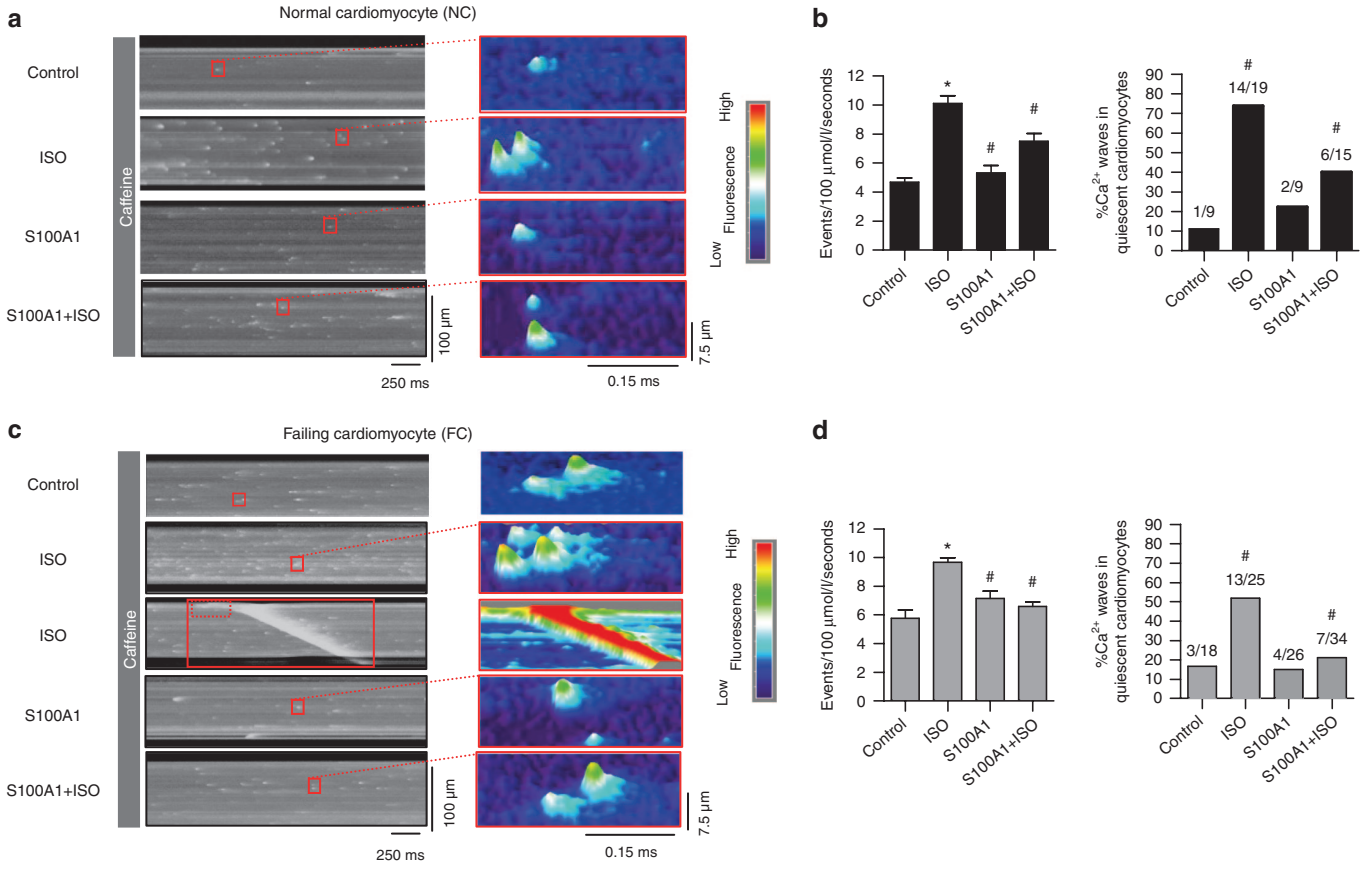

Figure 4 S100A1 prevents compound Ca^{2+} sparks and Ca^{2+} waves in quiescent ventricular cardiomyocytes with Ca^{2+} sensitized RyR2s. (**a**) and (**c**) Representative fluorescent line-scan and surface plot images of Ca^{2+} sparks in basal and ISO-stimulated (100 nmol/l) control (AdGFP) and S100A1-treated (AdS100A1) NCs (**a**) and FCs (**c**) with RyR2 sensitized to Ca^{2+} by low-dose (0.5 mmol/l) caffeine treatment. ISO triggers compound sparks and Ca^{2+} waves while S100A1-treatment entails solitary SR Ca^{2+} release events. Note that S100A1 inhibits the detrimental effects of ISO on SR Ca^{2+} leak. (**b**) and (**d**) Corresponding statistical analysis of Ca^{2+} spark frequency and Ca^{2+} wave incidence in NCs (**b**) and FCs (**d**) in indicated groups. $n = 40$ cells derived from four different isolations. $^{\#}P < 0.05$ versus ISO. Data are given as mean ± SEM.

Of note, S100A1-mediated protection occurred despite Ca^{2+}/CaMKII-induced alterations in RyR2 and PLB phosphorylation (**Supplementary Figure S6a–c**). Unchanged connexin-43 (Cx-43) phosphorylation and expression levels further corroborate improved RyR2 gating as underlying cause for the effect of S100A1 in electrically coupled cardiomyocytes (**Supplementary Figure S6d**). In the same manner, isoproterenol stimulation triggered diastolic premature contractions, whereas S100A1 overexpression efficiently protected against βAR-induced after-contractions (**Figure 6h,i**; **Supplementary Figure S6e**). Since these results support the point that S100A1 can protect electrically coupled cardiomyocytes against proarrhythmic SR Ca^{2+} leak despite CaMKII and PKA activation, we next investigated its potential to suppress catecholamine-triggered tachyarrhythmias in mice with postischemic HF *in vivo*.

S100A1 protects mice with postischemic heart failure against catecholamine-triggered ventricular tachyarrhythmias and death

To address this question, male C57BL/6 mice were subjected to left ventricular (LV) ischemia-reperfusion (I/R) injury (**Figure 7a**) and subsequently displayed significantly decreased contractility (**Figure 7b**) and diminished S100A1 protein expression (**Supplementary Figure S7a**). Intravenous injection of AAV9-S100A1 restored LV S100A1 expression and contractile indices were significantly improved (**Figure 7b**; **Supplementary Figure S7a,b**). Telemetric ECG monitoring recorded onset of ventricular fibrillation (VF) (**Figure 7c**) and death in response to acute epinephrine injection in AAV9-S100A1 and AAV9-GFP treated HF mice. VF occurred in 70% (14 out of 20) control mice of which 12 died (**Figure 7d**). Surviving animals converted to sinus rhythm after 30–45 minutes. AAV9-S100A1 treatment protected HF mice against epinephrine-triggered VF and death, respectively (**Figure 7d**). Although S100A1-treated mice responded with tachycardia or single ventricular extrasystoles to epinephrine injections as well (**Supplementary Figure S7c**), only 6 showed VF and only 4 died compared to 12 in the control group (**Figure 7d**). On a molecular level, epinephrine treatment showed the expected increase in RyR2 phosphorylation, which was unaffected by restored S100A1 expression (**Figure 7e**). Finally, AAV9-S100A1 gene transfer normalized the reduced binding of S100A1 to the RyR2 compared to AAV9-GFP control mice (**Figure 7f**). Our *in vivo* rescue corroborates S100A1 binding to the RyR2 as key for efficient diastolic RyR2 function and S100A1 overexpression sufficient to treat LV malfunction and ventricular arrhythmias *in vivo*.

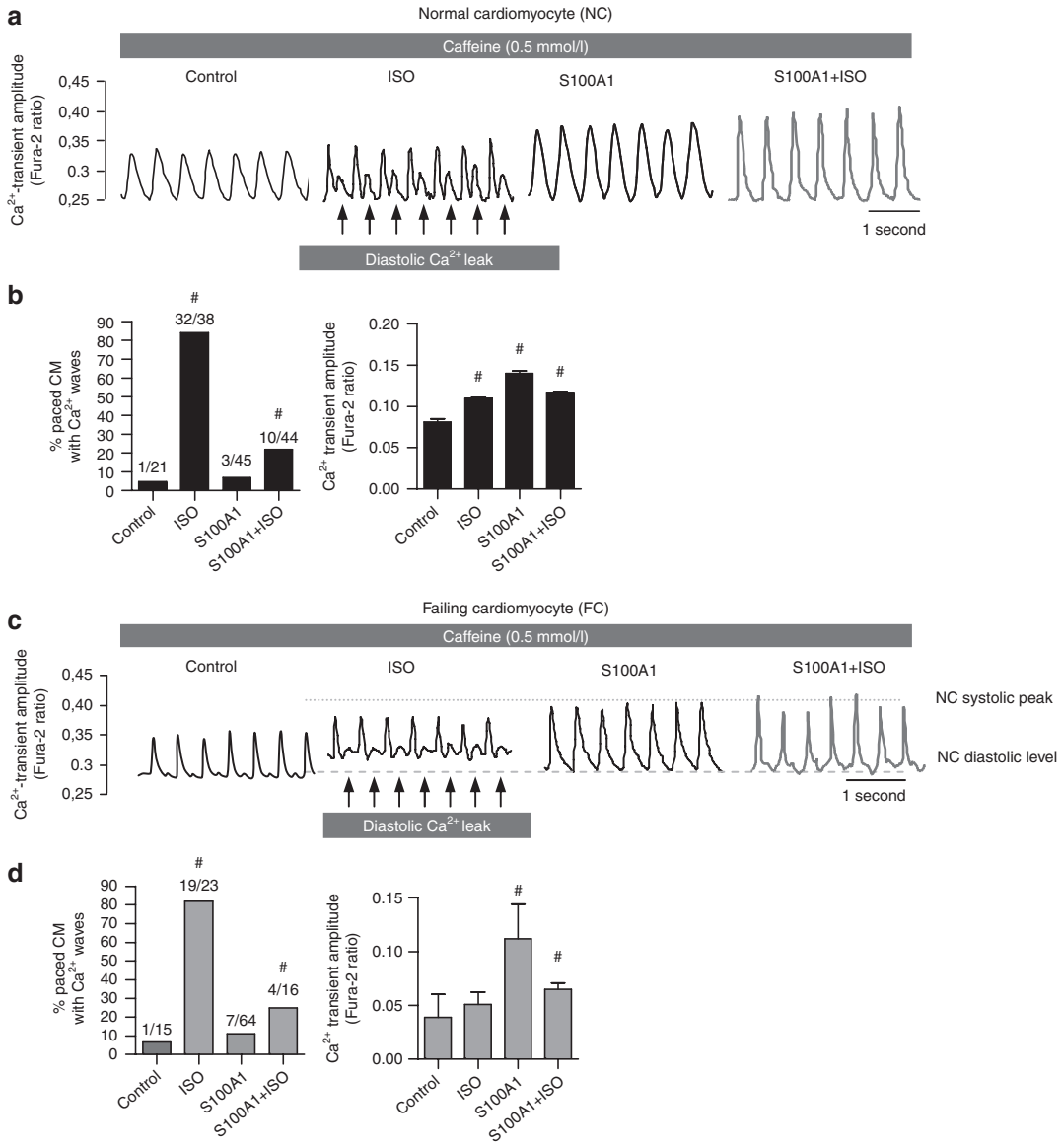

Figure 5 S100A1 prevents premature diastolic Ca^{2+} waves during EC coupling in electro-mechanically coupled ventricular cardiomyocytes with "leaky" RyR2. (**a**) and (**c**) Representative tracings of Ca^{2+} transients of electrically-paced and to Ca^{2+} sensitized RyR2s basal and ISO-stimulated (100 nmol/l) control (AdGFP) and S100A1-treated (AdS100A1) NCs (left) and FCs (right). (**b**) and (**d**) Statistical analysis of diastolic Ca^{2+} waves and systolic Ca^{2+} transient amplitudes in electrically paced NCs (b) and FCs (d). Number of cells analyzed per group is shown on top of each bar. $^{\#}P < 0.05$ versus ISO. Data are given as mean ± SEM.

DISCUSSION

This is the first report of a beneficial effect of S100A1 on RyR2-mediated SR Ca^{2+} leak in HF, which is spurred by the observation of a diminished interaction between both molecules in failing myocardium. Most salient finding of our study is that restoring this link can reverse diastolic RyR2 dysfunction and protect against proarrhythmic consequences of RyR2-mediated SR Ca^{2+} leak in failing myocardium *in vitro* and *in vivo*. The novel mechanism advances our understanding of S100A1's molecular mode of action in HF and bears relevance in view of S100A1-based therapeutics being translated toward clinical trials (reviewed in ref. [15]).

Key to this desirable effect might be the modulation of basal diastolic RyR2 function by S100A1 as shown in resting rat cardiomyocytes. Assessment of spontaneous elementary Ca^{2+} release events, independent of L-type Calcium channel activity, revealed S100A1-mediated attenuation of Ca^{2+} spark frequency in normal and failing cardiomyocytes. Although Ca^{2+} spark frequency was reduced after 24 hours of cultivation compared to freshly isolated CMs, which can be attributed to the culture period under unloaded conditions, this should not limit the significance of our results since we have used further approaches to determine RyR2 dysfunction *in vitro* and *in vivo*.

Our data is in line with previous reports showing attenuated RyR2 open probability by S100A1 in permeabilized cardiomyocytes and lipid bilayers studies at diastolic Ca^{2+} levels.[29,30] In contrast to βAR stimulation that exacerbated SR Ca^{2+} leak through enhanced Ca^{2+} sensitivity of the Ca^{2+} channel by PKA- and CaMKII-dependent phosphorylation,[7,10,31] S100A1 might

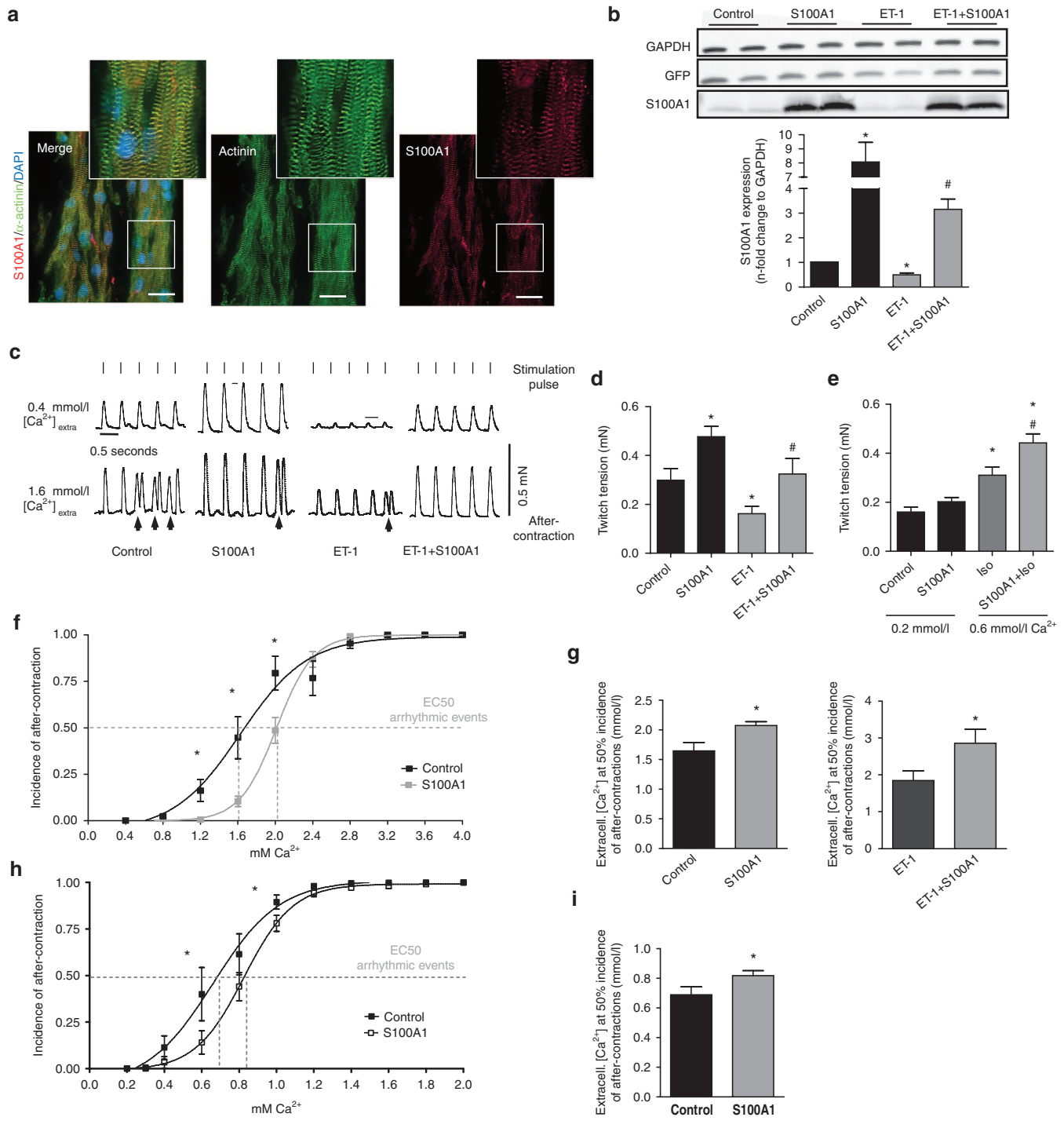

Figure 6 S100A1 restores isometric twitch tension and prevents premature diastolic after-contractions in engineered heart tissue (EHT). (**a**) Representative immunofluorescent staining displays a striated pattern of S100A1 (red) in cardiomyocytes in EHT. Cardiomyocytes were counter-stained with actinin (green) and 4',6-diamidino-2-phenylindole (DAPI) (nuclei, blue). Scale bar represents 20 µm. Inlet magnification is threefold. (**b**) Representative immunoblots for GFP and S100A1 from normal and ET-1 stimulated (ET-1, 40 nmol/l, 96 hours stimulation) control (AdGFP) or S100A1-treated (AdS100A1) EHTs. Quantification of S100A1 protein levels normalized to GAPDH is shown below. $n = 7$, $^{*}P < 0.05$ versus control, $^{\#}P < 0.05$ versus ET-1. (**c**) Representative electrically-stimulated isometric twitches from control- and S100A1-treated normal and HF-like EHT at 0.4 and 1.6 mmol/l extracellular Ca^{2+} ($[Ca^{2+}]_{extra}$). Lines indicate stimulation pulses (110 mA, 5 ms width, 2 Hz) inducing regular twitch; arrows indicate non-stimulated premature diastolic after-contractions. (**d**) Statistical analysis of twitch tension at 1.6 mmol/l $[Ca^{2+}]_{extra}$. $n = 19$ for control and S100A1, $n = 17$ for ET-1 and ET-1+S100A1, $^{*}P < 0.05$ versus control, $^{\#}P < 0.05$ versus ET-1. (**e**) Statistical analysis of twitch tension at 0.2 mmol/l and 0.6 $[Ca^{2+}]_{extra}$/1 µmol/l ISO. $n = 11$, $^{*}P < 0.05$ versus control. (**f**) Statistical analysis of premature diastolic after-contractions (in % of total twitches for each $[Ca^{2+}]_{extra}$) in control and S100A1-treated EHT. $n = 15$ for control and S100A1, $^{*}P < 0.05$ versus control. (**g**) Calculated EC 50% ($[Ca^{2+}]_{extra}$ at which 50% of EHTs shows regular after-contractions) in normal and ET-1 stimulated control and S100A1-treated EHT. $n = 15$ for control and S100A1, $n = 8$ for ET-1 and ET-1+S100A1; $^{*}P < 0.05$ versus control/ET-1. (**h**) Statistical analysis of premature diastolic after-contractions (in % of total twitches for each $[Ca^{2+}]_{extra}$) in control and S100A1-treated EHT after βAR stimulation. $n = 11$, $^{*}P < 0.05$ versus control. (**i**) Calculated EC 50% ($[Ca^{2+}]_{extra}$ at which 50% of EHTs shows regular after-contractions) in normal and S100A1 transfected EHT after βAR stimulation. $n = 11$, $^{*}P < 0.05$ versus control. Data are given as mean ± SEM.

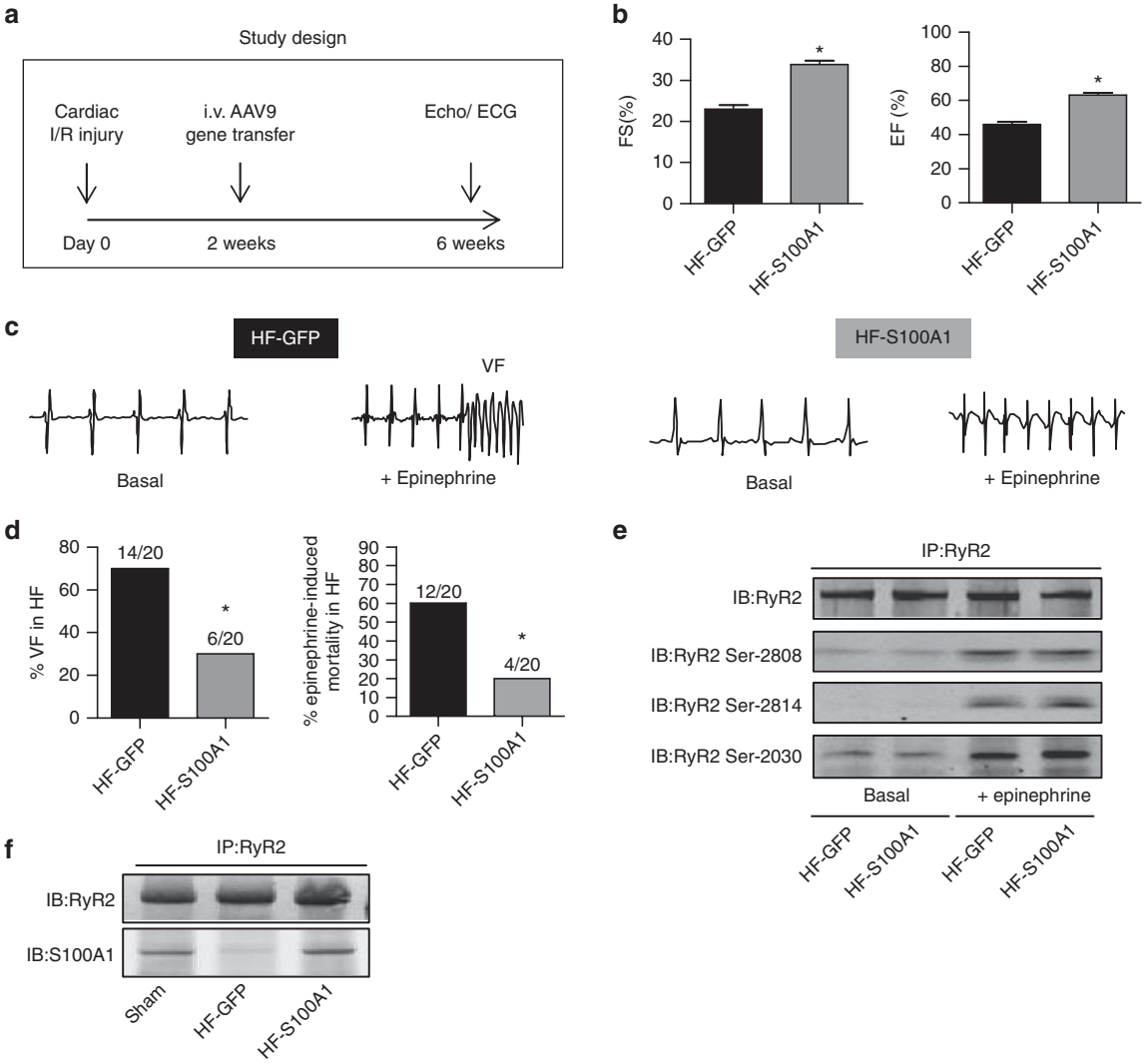

Figure 7 S100A1 protects against epinephrine-triggered ventricular tachyarrhythmias and death in postischemic failing mouse hearts *in vivo*. (**a**) Study protocol following cardiac ischemia-reperfusion (I/R) damage due to temporary LAD occlusion. (**b**) Quantification of basal contractile performance assessed by echocardiography in anesthetized mice (FS, fractional shortening; EF, ejection fraction) of HF-GFP and HF-S100A1 mice at 6 weeks. $n = 14$, $^*P < 0.05$ versus HF-GFP. (**c**) Representative telemetric ECG tracings of conscious HF mice (HF-GFP and HF-S100A1) depicting sinus rhythm before and development of ventricular fibrillation (VF) after i.p. injection of epinephrine (2 mg/kg body weight) in a HF-GFP mouse at week 6 of the study protocol. (**d**) Quantification of ventricular fibrillation (VF) and epinephrine-induced cardiac mortality in HF-GFP and HF-S100A1 mice. $n = 20$; $^*P < 0.05$ versus HF-GFP. (**e**) Representative phospho-specific immunoblots for Ser-2808, Ser-2814, and Ser-20130 sites of immunoprecipated RyR2 from indicated groups under basal conditions and 20 minutes after epinephrine treatment. The experiment was repeated four times with identical results. (**f**) Representative immunoblots of immunoprecipitated RyR2 and coprecipitating S100A1 protein from sham, HF-GFP, and HF-S100A1 murine myocardium at week 6 of the study protocol. Data are given as mean ± SEM.

attenuate Ca^{2+} responsiveness to a degree that prevents neighboring RyR2 recruitment within the same junction to induce a full-blown Ca^{2+} spark. Since SR Ca^{2+} content is elevated both in S100A1-treated normal and failing rat cardiomyocytes, our results further suggest that S100A1 might not only decrease cytosolic but also luminal Ca^{2+} sensitivity thereby enabling the channel to cope with increased SR Ca^{2+} load.[32] Continued studies are warranted to address this question. Our results obtained in resting cardiomyocytes with chemically sensitized RyR2s corroborate the perception of S100A1 as a potent negative allosteric regulator of diastolic RyR2 activity even under conditions where the diastolic Ca^{2+} leak is reinforced. High SR Ca^{2+} load, due to βAR stimulation, creates the condition where a Ca^{2+} spark in one junction triggers aberrant Ca^{2+} release at sensitized neighboring junctions (macrosparks), which in turn produces cell-wide arrhythmic Ca^{2+} waves.[2,33] S100A1, however, reduced the propensity for proarrhythmic Ca^{2+} waves indicating efficient inhibition of neighboring RyR2 recruitment under experimental conditions that closely approximate the HF state. The data derived from failing cardiomyocytes during EC coupling further strengthen the significance of our results: Restored S100A1/RyR2 binding almost completely abrogated premature diastolic Ca^{2+} waves in electrically-stimulated failing cardiomyocytes upon βAR stimulation. Due to preserved SR Ca^{2+} load, amplitudes of regular Ca^{2+} transients remained high. We could conclude that S100A1 improves RyR2 closure during diastole when the Ca^{2+} channel must shut off completely to allow

relaxation in order to proceed efficiently and to limit the amount of energetically futile SERCA2a activity compensating for the arrhythmic SR Ca^{2+} leak. These results also support the notion that this mechanism beneficially synergizes with enhanced SERCA2a activity thereby protecting against HF-related systolic and diastolic cardiomyocyte dysfunction. To better reflect characteristics of syncytial cardiac tissue, we evoked premature diastolic after-contractions in EHTs resulting from Ca^{2+}-induced SR Ca^{2+} overload in concert with increased CaMKII-activity. Reconstituted S100A1 expression rescued not only the HF-like phenotype but attenuated after-contractions and fibrillations in normal and HF-like EHTs under Ca^{2+}-/βAR-stress. In light of our previous results, restored S100A1/RyR2 interaction most likely accounts for enhanced resistance of electrically coupled cardiomyocytes against tissue-wide premature SR Ca^{2+} leak. Of note, connexin-43 expression and phosphorylation was unchanged, confirming that S100A1 did not interfere with current exchange between cardiomyocytes.[34] In keeping with previous studies, S100A1 reversed diastolic RyR2 dysfunction in several models despite persistent PKA- and CaMKII-dependent hyperphosphorylation. Our study might even indicate that disrupted S100A1/RyR2 interaction in HF is not the result of RyR2 hyperphosphorylation but rather follows diminution of S100A1 expression. In addition, S100A1 did not change stoichiometry of CaM with the RyR2 and vice versa, normalized S100A1 expression did not enhance association of CaM, FKBP12.6 or sorcin with the RyR2, each of which has been described to attenuate diastolic RyR2 activity.[2,10,31,35,36] This finding argues against competitive binding of S1001 and CaM, although recent reports alluded to putatively common binding sites of CaM and S100A1 at mutual targets.[30] Mapping, site-directed mutagenesis and quantitative binding studies are now required to locate interaction domains with the RyR2. Our study prompts further investigation of potential conformational changes within or between subunits of the RyR2. Overall, our data could lead to the assumption that improved S100A1/RyR2 interaction is sufficient to reverse diastolic RyR2 dysfunction in failing myocardium independent of its phosphorylation state and stoichiometry with assembled molecules. Therapeutic relevance of S100A1's antiarrhythmic potency was finally assessed in mice with post-I/R HF. Targeted restoration of cardiac S100A1 expression and interaction with the RyR2 *in vivo* was achieved by systemic AAV9-S100A1 delivery and use of a cardiomyocyte-specific promoter as previously reported.[37] S100A1-treated failing hearts were protected against catecholamine-induced tachyarrhythmias and death despite aberrant RyR2 phosphorylation at PKA- and CaMKII-targeted sites. Of note, S100A1 protein changes achieved by *in vitro* and *in vivo* cDNA delivery felt within the optimal therapeutic range.[38] Hence, our novel mechanistic data obtained in βAR-stimulated failing cardiomyocytes and EHTs strongly support the notion that S100A1 is necessary for diastolic RyR2 function *in vivo* and inhibits the occurrence of Ca^{2+}-triggered lethal fibrillation. As such, the Ca^{2+}-dependent inotrope S100A1 combines chronic cardiac performance enhancement with protection against Ca^{2+}-triggered arrhythmias. Given continued translation of an S100A1-based HF therapy toward clinical trials, our study unveils a novel molecular mechanism of S100A1 that could contribute to its favorable therapeutic profile. The pathophysiological relevance of altered RyR2 function in HF warrants continued investigation of S100A1's impact on the channel´s structure and function.

MATERIALS AND METHODS

A detailed description of materials and methods is available in the **Supplementary Materials and Methods**.

Experimental animal procedures. All animal procedures and experiments were performed in accordance with corresponding institutional guidelines of Thomas Jefferson University and University of Heidelberg.

Rat and mouse heart failure model. In 10–12-week-old male Sprague-Dawley rats HF was induced as described previously to receive isolated failing cardiomyocytes.[20] In mice, induction of myocardial ischemia/reperfusion injury (I/R) by temporary left anterior descending (LAD) coronary artery ligation was carried out in 7-week-old male C57BL/6 mice as described previously.[19,39]

Adenovirus and adeno-associated vector production. Adenovirus and AAV production was performed as described previously.[38]

Systemic in vivo adeno-associated virus serotype 9 gene transfer. Recombinant adeno-associated virus 9 (rAAV-9) gene transfer (1×10^{11} total viral particles) was carried out in mice 14 days after induction of MI as described previously.[37,40]

Telemetry. For telemetric electrocardiography (ECG) studies, radio frequency transmitters (ETA-F20; Data Sciences) were inserted subcutaneously into the back of HF mice as described previously.[41] Epinephrine (2 mg/kg body weight) was injected once intraperitoneal in conscious HF mice 4 weeks after AAV gene transfer.

Cardiomyocyte isolation and in vitro adenoviral gene transfer protocol. Cardiomyocytes were isolated from rat LV's 10-12 weeks after sham operation or infarction.[42]

Intracellular Ca^{2+} transients and sarcoplasmic reticulum Ca^{2+} load. Intracellular Ca^{2+} transients and SR Ca^{2+} load in Fura2-AM loaded adult normal and failing rat cardiomyocytes were measured as previously described.[29,42]

Ca^{2+} spark measurements. Ca^{2+} sparks in intact normal and failing adult rat cardiomyocytes were monitored using a Leica SP2, (Mannheim, Germany) laser scanning confocal microscope (LSCM) as described previously.[29] Recorded Ca^{2+} sparks were quantified using an automated algorithm adapted from a previously published method.[43]

Generation and cultivation of engineered heart tissue (EHT). Engineered heart tissue (EHT) was constructed as described previously.[19,44,45] After 7 days, EHTs were transferred onto custom-made stretch devices to facilitate phasic stretch (from 100 to 110% of length at 2 Hz). On day 8, EHTs were stimulated with endothelin (ET-1) (40 nmol/l) for 96 hours. Adenoviral transduction was performed for 48 hours in normal and ET-1 treated EHT with MOI 50, which resulted in a homogeneous GFP expression comparable in both vectors.

Isometric force analysis and arrhythmia assay. On day 12, isometric contraction experiments were performed in custom-designed organ bath apertures (Föhr Medical Instruments, Seeheim-Ober Beerbach, Germany). [Ca^{2+}] was increased stepwise after a recording period of 150 seconds. Data from three consecutive steady-state twitches were averaged for analysis of contractile performance. For the arrhythmia assay, the incidence of after-contractions and transition to fibrillation was counted manually for each calcium concentration as ratio number of after-contractions to total number of contractions.

Immunofluorescence (IF) staining, proximity ligation assay (PLA), immunoprecipitation, and western blotting. For detailed information, see **Supplementary Materials and Methods**.

Statistics. Data are generally expressed as mean ± SEM. An unpaired two-tail student's *t*-test, one-way ANOVA or two-way repeated measures ANOVA were performed for statistical comparisons unless indicated otherwise. A P value of <0.05 was considered significant.

SUPPLEMENTARY MATERIAL

Figure S1. Characterization of myocardial infarction model 2 weeks after LAD ligation.
Figure S2. AdS100A1 treatment of normal and failing rat cardiomyocytes.
Figure S3. S100A1 does not alter PLB phosphorylation nor RyR2 interaction with accessory proteins.
Figure S4. Low-dose caffeine does not change binding of S100A1 to the RyR2.
Figure S5. S100A1 rescues HF-like EHT contractility and Ca^{2+} responsiveness and Ca^{2+} stress leads to the development of premature diastolic contractions (after-contractions) in EHT.
Figure S6. S100A1 overexpression does not modulate CamKII activity and Connexin43 expression in arrhythmic EHTs.
Figure S7. S100A1 protects against epinephrine-triggered ventricular tachycardia in postischemic failing mouse hearts *in vivo*.

ACKNOWLEDGMENTS

We thank Nicole Herzog and Jasmin Hoffmann for excellent technical assistance. This study was supported by grants of the National Institute of Health (RO1 HL92130 and RO1HL92130-02S1 to P.M.; PO1 HL075443 (Project 2), RO1 HL56205 and RO1 HL061690 to W.J.K.), the Deutsche Forschungsgemeinschaft (562/1-1 to P.M. and S.T.P., 1659/1-1 to M.V.), Bundesministerium für Bildung und Forschung (01GU0572 to P.M.) and grants from the German Cardiovascular Research Center (DZHK, to P.M. and H.A.K.). P.M. and H.A.K. hold patents on the therapeutic use of S100A1 in cardiovascular diseases. P.M. and H.A.K. are shareholders of UniQure N.K.

REFERENCES

1. Bers, DM (2002). Cardiac excitation-contraction coupling. *Nature* **415**: 198–205.
2. Bers, DM (2014). Cardiac sarcoplasmic reticulum calcium leak: basis and roles in cardiac dysfunction. *Annu Rev Physiol* **76**: 107–127.
3. Morgan, JP, Erny, RE, Allen, PD, Grossman, W and Gwathmey, JK (1990). Abnormal intracellular calcium handling, a major cause of systolic and diastolic dysfunction in ventricular myocardium from patients with heart failure. *Circulation* **81**(2 Suppl): III21–III32.
4. Farr, MA and Basson, CT (2004). Sparking the failing heart. *N Engl J Med* **351**: 185–187.
5. Katz, AM (1986). Potential deleterious effects of inotropic agents in the therapy of chronic heart failure. *Circulation* **73**(3 Pt 2): III184–III190.
6. Overgaard, CB and Dzavík, V (2008). Inotropes and vasopressors: review of physiology and clinical use in cardiovascular disease. *Circulation* **118**: 1047–1056.
7. Eisner, DA, Kashimura, T, Venetucci, LA and Trafford, AW (2009). From the ryanodine receptor to cardiac arrhythmias. *Circ J* **73**: 1561–1567.
8. Venetucci, LA, Trafford, AW and Eisner, DA (2007). Increasing ryanodine receptor open probability alone does not produce arrhythmogenic calcium waves: threshold sarcoplasmic reticulum calcium content is required. *Circ Res* **100**: 105–111.
9. Pogwizd, SM, Schlotthauer, K, Li, L, Yuan, W and Bers, DM (2001). Arrhythmogenesis and contractile dysfunction in heart failure: Roles of sodium-calcium exchange, inward rectifier potassium current, and residual beta-adrenergic responsiveness. *Circ Res* **88**: 1159–1167.
10. Marx, SO and Marks, AR (2013). Dysfunctional ryanodine receptors in the heart: new insights into complex cardiovascular diseases. *J Mol Cell Cardiol* **58**: 225–231.
11. George, CH, Jundi, H, Thomas, NL, Fry, DL and Lai, FA (2007). Ryanodine receptors and ventricular arrhythmias: emerging trends in mutations, mechanisms and therapies. *J Mol Cell Cardiol* **42**: 34–50.
12. Ter Keurs, HE and Boyden, PA (2007). Calcium and arrhythmogenesis. *Physiol Rev* **87**: 457–506.
13. Eisner, DA, Kashimura, T, O'Neill, SC, Venetucci, LA and Trafford, AW (2009). What role does modulation of the ryanodine receptor play in cardiac inotropy and arrhythmogenesis? *J Mol Cell Cardiol* **46**: 474–481.
14. Venetucci, LA, Trafford, AW, O'Neill, SC and Eisner, DA (2008). The sarcoplasmic reticulum and arrhythmogenic calcium release. *Cardiovasc Res* **77**: 285–292.
15. Pleger, ST, Brinks, H, Ritterhoff, J, Raake, P, Koch, WJ, Katus, HA *et al.* (2013). Heart failure gene therapy: the path to clinical practice. *Circ Res* **113**: 792–809.
16. Ritterhoff, J and Most, P (2012). Targeting S100A1 in heart failure. *Gene Ther* **19**: 613–621.
17. Rohde, D, Ritterhoff, J, Voelkers, M, Katus, HA, Parker, TG and Most, P (2010). S100A1: a multifaceted therapeutic target in cardiovascular disease. *J Cardiovasc Transl Res* **3**: 525–537.
18. Brinks, H, Rohde, D, Voelkers, M, Qiu, G, Pleger, ST, Herzog, N *et al.* (2011). S100A1 genetically targeted therapy reverses dysfunction of human failing cardiomyocytes. *J Am Coll Cardiol* **58**: 966–973.
19. Most, P, Seifert, H, Gao, E, Funakoshi, H, Völkers, M, Heierhorst, J *et al.* (2006). Cardiac S100A1 protein levels determine contractile performance and propensity toward heart failure after myocardial infarction. *Circulation* **114**: 1258–1268.
20. Most, P, Pleger, ST, Völkers, M, Heidt, B, Boerries, M, Weichenhan, D *et al.* (2004). Cardiac adenoviral S100A1 gene delivery rescues failing myocardium. *J Clin Invest* **114**: 1550–1563.
21. Remppis, A, Greten, T, Schäfer, BW, Hunziker, P, Erne, P, Katus, HA *et al.* (1996). Altered expression of the Ca(2+)-binding protein S100A1 in human cardiomyopathy. *Biochim Biophys Acta* **1313**: 253–257.
22. Pleger, ST, Most, P, Boucher, M, Soltys, S, Chuprun, JK, Pleger, W *et al.* (2007). Stable myocardial-specific AAV6-S100A1 gene therapy results in chronic functional heart failure rescue. *Circulation* **115**: 2506–2515.
23. Pleger, ST, Shan, C, Ksienzyk, J, Bekeredjian, R, Boekstegers, P, Hinkel, R *et al.* (2011). Cardiac AAV9-S100A1 gene therapy rescues post-ischemic heart failure in a preclinical large animal model. *Sci Transl Med* **3**: 92ra64.
24. Pleger, ST, Kziencek, J, Mueller, O, Bekeredjian, R, Remppis, A (2008). Retroinfusion-facilitated inotropic AAV9-S100A1 gene therapy restores global cardiac function in a clinically relevant pig heart failure model. *Circulation* **118**: S_792.
25. Pleger, ST, Remppis, A, Heidt, B, Völkers, M, Chuprun, JK, Kuhn, M *et al.* (2005). S100A1 gene therapy preserves *in vivo* cardiac function after myocardial infarction. *Mol Ther* **12**: 1120–1129.
26. Kettlewell, S, Most, P, Currie, S, Koch, WJ and Smith, GL (2005). S100A1 increases the gain of excitation-contraction coupling in isolated rabbit ventricular cardiomyocytes. *J Mol Cell Cardiol* **39**: 900–910.
27. Most, P, Boerries, M, Eicher, C, Schweda, C, Völkers, M, Wedel, T *et al.* (2005). Distinct subcellular location of the Ca2+-binding protein S100A1 differentially modulates Ca2+-cycling in ventricular rat cardiomyocytes. *J Cell Sci* **118**(Pt 2): 421–431.
28. Most, P, Remppis, A, Pleger, ST, Löffler, E, Ehlermann, P, Bernotat, J *et al.* (2003). Transgenic overexpression of the Ca2+-binding protein S100A1 in the heart leads to increased *in vivo* myocardial contractile performance. *J Biol Chem* **278**: 33809–33817.
29. Völkers, M, Loughrey, CM, Macquaide, N, Remppis, A, DeGeorge, BR Jr, Wegner, FV *et al.* (2007). S100A1 decreases calcium spark frequency and alters their spatial characteristics in permeabilized adult ventricular cardiomyocytes. *Cell Calcium* **41**: 135–143.
30. Yamaguchi, N, Chakraborty, A, Huang, TQ, Xu, L, Gomez, AC, Pasek, DA *et al.* (2013). Cardiac hypertrophy associated with impaired regulation of cardiac ryanodine receptor by calmodulin and S100A1. *Am J Physiol Heart Circ Physiol* **305**: H86–H94.
31. Marx, SO, Reiken, S, Hisamatsu, Y, Jayaraman, T, Burkhoff, D, Rosemblit, N *et al.* (2000). PKA phosphorylation dissociates FKBP12.6 from the calcium release channel (ryanodine receptor): defective regulation in failing hearts. *Cell* **101**: 365–376.
32. Györke, I and Györke, S (1998). Regulation of the cardiac ryanodine receptor channel by luminal Ca2+ involves luminal Ca2+ sensing sites. *Biophys J* **75**: 2801–2810.
33. Cheng, H and Lederer, WJ (2008). Calcium sparks. *Physiol Rev* **88**: 1491–1545.
34. Lampe, PD and Lau, AF (2004). The effects of connexin phosphorylation on gap junctional communication. *Int J Biochem Cell Biol* **36**: 1171–1186.
35. Farrell, EF, Antaramian, A, Rueda, A, Gómez, AM and Valdivia, HH (2003). Sorcin inhibits calcium release and modulates excitation-contraction coupling in the heart. *J Biol Chem* **278**: 34660–34666.
36. Xu, L and Meissner, G (2004). Mechanism of calmodulin inhibition of cardiac sarcoplasmic reticulum Ca2+ release channel (ryanodine receptor). *Biophys J* **86**: 797–804.
37. Völkers, M, Weidenhammer, C, Herzog, N, Qiu, G, Spaich, K, von Wegner, F *et al.* (2011). The inotropic peptide ßARKct improves ßAR responsiveness in normal and failing cardiomyocytes through G(ß?)-mediated L-type calcium current disinhibition. *Circ Res* **108**: 27–39.
38. Weber, C, Neacsu, I, Krautz, B, Schlegel, P, Sauer, S, Raake, P *et al.* (2014). Therapeutic safety of high myocardial expression levels of the molecular inotrope S100A1 in a preclinical heart failure model. *Gene Ther* **21**: 131–138.
39. Tsuda, T, Gao, E, Evangelisti, L, Markova, D, Ma, X and Chu, ML (2003). Post-ischemic myocardial fibrosis occurs independent of hemodynamic changes. *Cardiovasc Res* **59**: 926–933.
40. Müller, OJ, Schinkel, S, Kleinschmidt, JA, Katus, HA and Bekeredjian, R (2008). Augmentation of AAV-mediated cardiac gene transfer after systemic administration in adult rats. *Gene Ther* **15**: 1558–1565.
41. Mitchell, GF, Jeron, A and Koren, G (1998). Measurement of heart rate and Q-T interval in the conscious mouse. *Am J Physiol* **274**(3 Pt 2): H747–H751.
42. Most, P, Bernotat, J, Ehlermann, P, Pleger, ST, Reppel, M, Börries, M *et al.* (2001). S100A1: a regulator of myocardial contractility. *Proc Natl Acad Sci USA* **98**: 13889–13894.
43. Cheng, H, Song, LS, Shirokova, N, González, A, Lakatta, EG, Ríos, E *et al.* (1999). Amplitude distribution of calcium sparks in confocal images: theory and studies with an automatic detection method. *Biophys J* **76**: 606–617.
44. Zimmermann, WH, Schneiderbanger, K, Schubert, P, Didié, M, Münzel, F, Heubach, JF *et al.* (2002). Tissue engineering of a differentiated cardiac muscle construct. *Circ Res* **90**: 223–230.
45. Tiburcy, M, Didié, M, Boy, O, Christalla, P, Döker, S, Naito, H *et al.* (2011). Terminal differentiation, advanced organotypic maturation, and modeling of hypertrophic growth in engineered heart tissue. *Circ Res* **109**: 1105–1114.